Volume 2 | Number 12 | December 2015

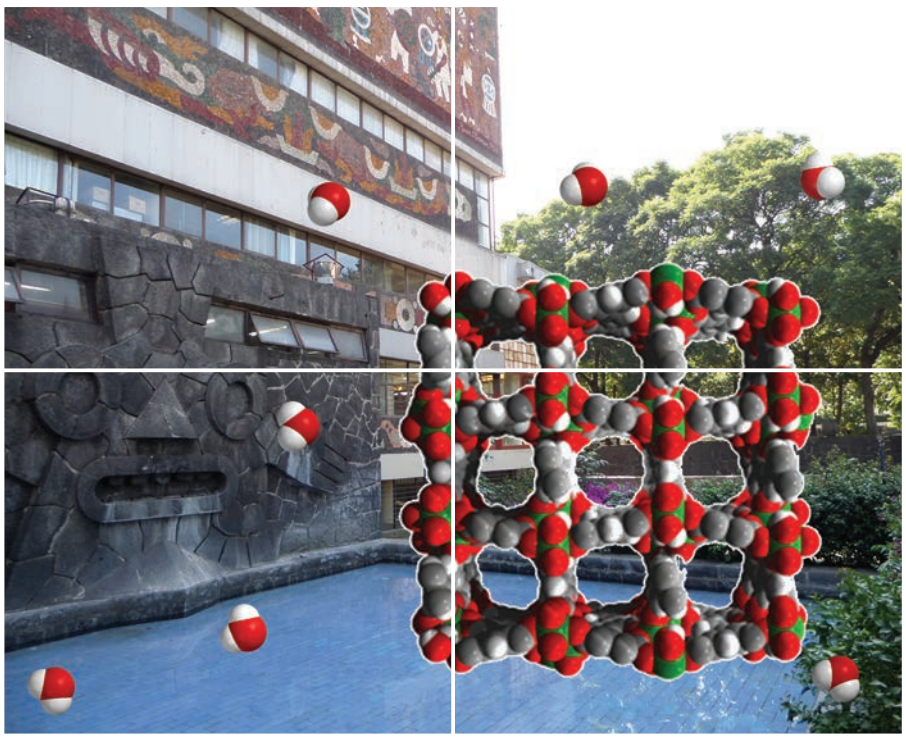

INORGANIC CHEMISTRY

FRONTIERS

Chinese Chemical Society
PEKING UNIVERSITY 1898
ROYAL SOCIETY OF CHEMISTRY

http://rsc.li/frontiers-inorganic

INORGANIC CHEMISTRY
FRONTIERS

RESEARCH ARTICLE

View Article Online
View Journal | View Issue

Cite this: *Inorg. Chem. Front.*, 2015, **2**, 1080

Water adsorption properties of a Sc(III) porous coordination polymer for CO_2 capture applications†‡

J. Raziel Álvarez,[a] Ricardo A. Peralta,[a] Jorge Balmaseda,[a] Eduardo González-Zamora*[b] and Ilich A. Ibarra*[a]

Received 9th September 2015,
Accepted 30th October 2015

DOI: 10.1039/c5qi00176e

rsc.li/frontiers-inorganic

Water adsorption at room temperature in NOTT-400 was investigated along with its ability to perform CO_2 capture under relative humidity (RH) conditions. Thus, the CO_2 capture was increased from 4.2 wt% (anhydrous conditions) to 10.2 wt% at 20% RH and 30 °C.

Metal–organic frameworks (MOFs) or porous coordination polymers (PCPs) are very promising candidates for gas sequestration, since these materials show high sorption selectivity towards adsorbates. This selectivity can be adjusted as a function of the size, shape and chemical composition of the pores.[1] Even with their potential as porous capture materials, many PCPs are unstable when exposed to moisture.[2,3] Water could either shift the bound ligand, leading to the collapse of the PCP structure, or block the binding adsorption sites and therefore, avoid the adsorption of other desired molecules.[3] Thus, water stability has limited the use of PCPs in industrial settings because moisture is ubiquitous in the environment and it must be accounted for in adsorption, storage and separation systems. For example, natural gas streams are frequently saturated with water vapour that has to be removed (to ppm levels) before storage or use.[4] Industrial flue gas, resulting from the combustions of fossil fuels, is saturated with water (5–7%).[5]

However, a significant number of PCPs have exhibited relatively good stability to water, for example: UiO-66,[6] NOTT-401,[7] MIL-100,[8] MIL-101,[9] MIL-53[10] and InOF-1.[11] Thus, understanding and predicting the adsorption properties of water in hydrostable PCPs is fundamental for the development of industrial applications. Doonan and co-workers[12] showed a Cu(II) metal–organic framework (Cu(bcppm)H_2O, H_2bcppm = bis(4-(4-carboxyphenyl)-1*H*-pyrazolyl)methane) which is hydrostable and also performed a remarkable selective separation of CO_2 from N_2. Walton and co-workers have shown water adsorption isotherms for a series of PCPs (Mg-MOF-174, DMOF-1, UiO-66 and UMCM-1) and compared them with reference micro-mesoporous materials.[13] Farrusseng *et al.*[14] reported the structure property relationships of water adsorption in a comprehensive series of PCPs (MIL-53, MIL-68, MIL-101, MIL-125, *etc.*). Moreover, some of these water stable materials have been investigated for application in storage technologies for arid environments,[15] heat-pumps and chillers,[16] low-cost water capture[15] and proton conductivity.[17]

The effect of water on the CO_2 capture has only recently been investigated on PCPs.[18] Water adsorption is often unfavourable for CO_2 capture since water acts as a strong adsorptive competitor. However, LeVan,[19] Matzger[20] and Walton[21] demonstrated that controlled water adsorption can enhance CO_2 capture in PCPs. Llewellyn and co-workers[22] investigated the CO_2 adsorption in some PCPs under different relative humidities of water vapour. Then, UiO-66 did not show any enhanced CO_2 uptake and for MIL-100(Fe), a remarkable 5-fold increase in CO_2 uptake was achieved. Interestingly, Walton and co-workers[23] showed that functional groups act as a directing agent for water in the pores, which allows for more efficient packing. Furthermore, Yaghi *et al.*[15] proposed that the presence of these functional groups, within the porous coordination polymer, enhance the affinity of the material for water. Thus, in the present work we have chosen a material named NOTT-400.[24a] This material crystallises in the tetragonal space group $I4_122$, showing a binuclear [$Sc_2(\mu_2$-OH)] building block (Fig. S1, ESI‡). The coordination around each Sc(III) centre is octahedral from six O-donors: 4 from different carboxylate groups and 2 from two μ_2-OH hydroxo groups which bridge two metal (Sc(III)) centres. NOTT-400 shows a three-dimensional framework structure with channel openings of approximately 8.1 Å (considering the van

[a]*Instituto de Investigaciones en Materiales, Universidad Nacional Autónoma de México, Circuito Exterior s/n, CU, Del. Coyoacán, 04510 México D. F., Mexico. E-mail: argel@unam.mx*
[b]*Departamento de Química, Universidad Autónoma Metropolitana-Iztapalapa, San Rafael Atlixco 186, Col. Vicentina, Iztapalapa, C. P. 09340, México D. F., Mexico*

†Dedicated to Professor Pedro Bosch who contributed with 38 years of brilliant research.

‡Electronic supplementary information (ESI) available: TGA data, PXRD data and kinetic CO_2 experiments. See DOI: 10.1039/c5qi00176e

der Waals radii of the surface atoms).[24a] We report herein the water adsorption properties and the CO_2 capture in the presence of water[24b] in NOTT-400.

First, the non-coordinated solvent molecules within the pores of the as-synthesised NOTT-400 were exchanged for acetone promoting accessibility to the desolvated framework after activation by heating. Thermogravimetric analysis (see Fig. S2, ESI‡) and bulk powder X-ray diffraction (PXRD) patterns (see Fig. S3, ESI‡) of the as-synthesised and desolvated NOTT-400 confirmed that the material constantly maintains its structural integrity after desolvation. N_2 adsorption isotherms for activated NOTT-400 at 77 K were obtained in order to calculate the BET surface area ($0.01 < P/P_0 < 0.04$) of 1356 $m^2\ g^{-1}$ (see Fig. S8, ESI‡). Water isotherms were obtained on the activated samples of NOTT-400 (see the Experimental section). Fig. 1 shows the water adsorption isotherm of NOTT-400 at 30 °C. The adsorbed amount of water slowly increased with increasing pressure up to $\%P/P_0 = 20$. Thus, a rapid water uptake was observed in the pressure range from $\%P/P_0 = 20$ to 40. Finally, from $\%P/P_0 = 40$ to 90 there was a gradual weight increase, and the maximum water uptake was ~44.9 wt%. The overall water isotherm exhibited a sigmoidal shape and a relatively strong hysteresis loop (at $\%P/P_0 = 20$–80) was observed with marked stepped profiles in the desorption phase (Fig. 1, open circles).

The pore openings in NOTT-400 (approximately 8.1 Å)[24a] are considerably much larger than the kinetic diameter of water (~2.7 Å). Thus, in order to interpret this hysteresis loop, the arguments of 'kinetic trap', suggested by other research groups,[25] seem not to be suitable. Instead, the observed hysteresis is most likely due to moderately strong host–guest interactions, which result in an enhanced affinity of NOTT-400 for water. We believe that such interactions arise from the fact that water molecules can form hydrogen bonds with the bridging hydroxo functional groups (μ_2-OH), within the pores, as previously described.[26]

In addition, according to the crystal structure of NOTT-400[24a] there are 8 hydroxo groups (μ_2-OH) per unit cell. Thus, at low water loadings these groups can interact with water molecules representing the first domain (from 0 to approximately 32% P/P_0) of the water adsorption isotherm. The second domain, after the full coverage of the hydroxo functional groups with H_2O molecules, occurs at higher loadings. Thus, the slope of the isotherm grew abruptly due to stronger intermolecular interactions between water molecules affording the condensation of water into the pores (Fig. S5, see ESI‡).

In order to measure the isosteric heat of adsorption for H_2O, we recorded a water adsorption isotherm at 20 °C (see Fig. S9, ESI‡) and the enthalpy for H_2O adsorption was then calculated by fitting both isotherms (30 and 20 °C) to a Clausius–Clapeyron equation (see ESI‡). The estimated enthalpy value was 46.8 kJ mol^{-1} which is a typical value for PCPs.[21d]

To test the water adsorption–desorption recyclability of NOTT-400 water sorption isotherms were measured, on the same sample, for 5 cycles at 30 °C (Fig. 2). These results showed no apparent decrease in capacity over five cycles and revealed the complete regeneration of the material solely by evacuating for only 30 min without any thermal activation. In order to investigate any sample degradation, we have carried out PXRD experiments on the NOTT-400 sample after these cycling experiments. Fig. S4 (see ESI‡) confirms that the crystallinity of the sample after each water adsorption–desorption experiment (5 cycles) was retained.

Dynamic and isothermal CO_2 experiments were performed on NOTT-400 (see the Experimental section). In Fig. 3, a kinetic uptake experiment at 30 °C is shown. At this ambient temperature, the maximum amount of CO_2 captured under anhydrous conditions is 4.4 wt%, rapidly reached after only 7 min and it was constant until the end of the experiment at 60 min. In addition, we run CO_2 sorption experiments (adsorp-

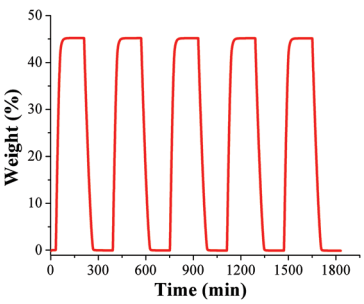

Fig. 2 Water readsorption–desorption uptake on NOTT-400 at 30 °C.

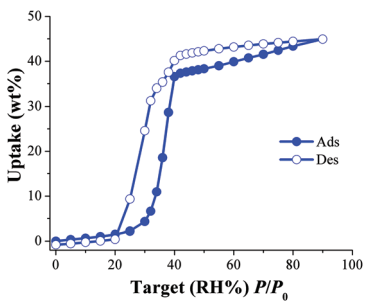

Fig. 1 Water adsorption isotherm at 30 °C of NOTT-400. Solid circles represent adsorption, and open circles show desorption.

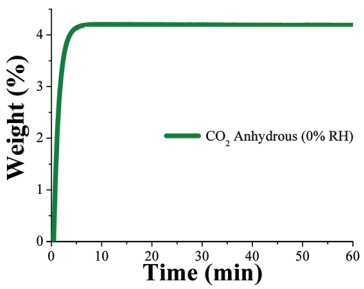

Fig. 3 Kinetic uptake experiment performed at 30 °C with a CO_2 flow of 60 mL min^{-1}.

tion/desorption) under static and isothermal conditions on NOTT-400 (see Fig. S10, ESI‡). The CO_2 capture was 18.2 wt% which is significantly higher than under dynamic conditions (4.4 wt%). However, the central target of this paper is to exhibit, in a more realistic scenario, how NOTT-400 performs when it is exposed to a constant CO_2 flow gas (60 mL min^{-1}) and under water conditions.

Kinetic isotherm experiments at 30 °C and different relative humidities (10, 20, 35 and 60% RH) were carried out. We decided on these RH values based on the water adsorption isotherm (see Fig. 1): two values in the low loading region (10 and 20% RH); one value in the middle of the sigmoidal-shaped isotherm (35% RH) and finally one value in the high loading region (60% RH). First, an activated NOTT-400 sample (180 °C for 1 h and under a flow of N_2 gas) was stabilised at 30 °C and 10% RH. After the equilibrium was reached a constant CO_2 flow (60 mL min^{-1}) was carried out (see Fig. 4, left).

In Fig. 4 (left) the gradual weight increase (only H_2O) starts at 0 min and is stabilised at around 15 min. In contrast, under anhydrous conditions the CO_2 uptake quickly reached stability (7 min, see Fig. 3). Since the diffusion coefficient of water is smaller than CO_2, the vapour adsorption (water) process takes considerably more time to stabilise than the gas adsorption process in microporous materials.[27] Then, from 15 min to 50 min the H_2O uptake (0.7 wt%, which is in good agreement with the water adsorption isotherm; 0.67 wt%) was constant (plateau) and next, at 50 min the CO_2 flow (60 mL min^{-1}) was opened and a sharp weight gain, which reached stability at approximately 70 min, was observed (see Fig. 4, left). We hypothesise that the adsorbed amount of H_2O is unchanged after the dosing of H_2O/CO_2 mixed gas, as we observed earlier.[29] Then, from 70 min to 120 min (end of the experiment), the maximum amount of CO_2 captured (considering the water uptake of 0.7 wt%) corresponded to 7.8 wt%. Therefore, the CO_2 capture was approximately 2-fold increased with a 10% RH (from 4.2 wt% to 7.8 wt%) in comparison with anhydrous conditions.

Later, kinetic CO_2 uptake experiments were performed on an activated sample of NOTT-400 at 30 °C and 20% RH. Fig. 4 (right) shows the gradual weight increase (H_2O) starting at 0 min and stabilised at around 15 min. From 15 to 50 min the water uptake was constant and equal to 1.5 wt% (in good agreement with the water adsorption isotherm value of 1.47 wt%).

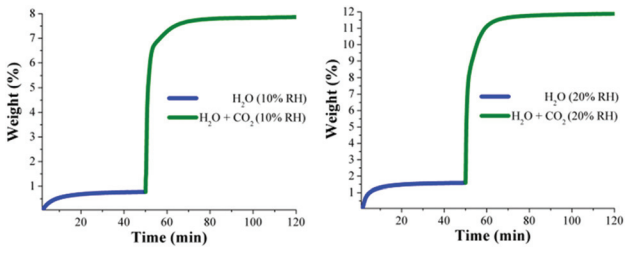

Fig. 4 Kinetic uptake experiments carried out at 10 and 20% RH (both experiments at 30 °C); H_2O (blue line) and H_2O + CO_2 (green line).

Then, the CO_2 flow was opened and abrupt uptake was observed (Fig. 4 right). After stabilisation (after 70 min) the total CO_2 uptake was equal to 10.2 wt%. Thus, the CO_2 capture was approximately 2.5-fold increased (from anhydrous conditions to 20% RH). This enhance in the CO_2 uptake in the presence of water can be explained by CO_2 confinement effects induced by water molecules.[28]

Similarly, more kinetic CO_2 uptake isotherm experiments were carried out on the activated samples of NOTT-400 at 30 °C and 35% RH (see Fig. S6, ESI‡) and 30 °C and 60% RH (see Fig. S7, ESI‡). The stabilisation times were 40 and 55 min (see Fig. S6 and S7, ESI‡), respectively, and in both cases after the CO_2 flow was started there was no weight increase, meaning that CO_2 capture was not achieved at those relative humidities. At 35 and 60% RH, the water uptakes were 18.6 and 39.9 wt%, respectively. These values were in good agreement with the water adsorption isotherms (see Fig. 1), 18.72 and 39.88 wt%, respectively.

The porosity of NOTT-400 corresponds to the microporosity regime with a pore diameter of 8.1 Å.[24a] The remarkable result shown by Llewellyn and co-workers,[22] increase in the CO_2 uptake, was reported in a mesoporous material at 40% RH and 30 °C (MIL-100(Fe)).[22] This mesoporous material includes two types of cages of free openings of ~25 and 29 Å.[22] We elucidated that at 35 and 60% RH the saturation of the micropores in NOTT-400, with H_2O molecules, was complete and thus, the inclusion of CO_2 molecules, into the micropores, was not possible. This explanation is supported by the experimental evidence that we previously reported[29] in another microporous material.

Additionally, Paesani *et al.*[30] investigated by computational infrared spectroscopy the behavior of water confined in a porous coordination polymer named MIL-53(Cr).[31] Interestingly, MIL-53(Cr) is constructed with one-dimensional chains of corner-sharing $CrO_4(\mu_2\text{-OH})$ octahedra, linked by 1,4-benzenedicarboxylate (BDC) ligands.[31] Thus, they demonstrated[30] that water molecules (at low water loadings) interact strongly with the framework, *via* hydrogen bonding between the μ_2-OH functional group and H_2O, whereas intermolecular interactions between H_2O molecules become considerably stronger at higher loading. In other words, at low water loadings the MIL-53(Cr) channels provide a template for more efficiently packing the water molecules and therefore, these H_2O molecules can then donate a hydrogen bond to the CO_2 molecules enhancing the total CO_2 uptake. These results correlate and support our experimental evidence.

Conclusions

In summary, the hydrostable Sc(III) coordination polymer, NOTT-400, has enabled an evaluation of how porous coordination polymers can be used in the sorption of water at ambient temperature. NOTT-400 carries out CO_2 sequestration under relative humidity conditions. Finding the best partial saturation of H_2O molecules (percentage of relative humidity)

into the micropores of NOTT-400 is crucial to increase the CO_2 uptake. Thus, after testing different relative humidity conditions (60, 35, 20 and 10% RH), we found that the maximum CO_2 capture was obtained at 20% RH and 30 °C with a total amount of ~10.2 wt%. Considerably, this CO_2 capture, under humid conditions, represents a 2.5-fold increase in comparison with anhydrous conditions. The CO_2 confinement effects induced by H_2O[28] can occur within the micropores of NOTT-400 enhancing the total CO_2 uptake.

Experimental section

Water adsorption experiments

Water vapour isotherms were recorded by a dynamic method, using air as a carrier gas, in a DVS Advantage 1 instrument from a surface measurement system (mass sensitivity: 0.1 μg, Relative Humidity (RH), accuracy: 0.5% RH, vapour pressure accuracy: 0.7% P/P_0). The hydration–dehydration cycles were measured in the same instrument. The water uptake in weight percent (wt%) units was calculated as [(adsorbed amount of water)/(amount of adsorbent) × 100], consistent with the established procedures.

CO_2 capture experiments

Kinetic uptake experiments were performed by using a thermobalance (Q500 HR, from TA) at room temperature (30 °C) with a constant CO_2 flow (60 mL min^{-1}). Then, samples of NOTT-400 were placed inside the thermobalance and activated by heating from room temperature to 180 °C for 1 h under a flow of N_2 gas. After the activated sample was cooled down, the desired temperature was set (30 °C) and a constant CO_2 flow (60 mL min^{-1}) was carried out. With a humidity-controlled thermobalance (Q5000 SA, from TA) kinetic uptake experiments at 30 °C with a constant CO_2 flow (60 mL min^{-1}) were performed on the activated samples (180 °C for 1 h under a flow of N_2 gas) of NOTT-400.

Acknowledgements

The authors thank Dr A. Tejeda-Cruz (X-ray; IIM-UNAM), CONACyT Mexico (212318), and PAPIIT UNAM Mexico (IN100415) for financial support. J. B. thanks SEP-CONACyT (154626) and UNAM-DGAPA-PAPIIT (IG-100315). E.G-Z. thanks CONACyT (156801 and 236879), Mexico for financial support. Thanks to U. Winnberg (ITAM and ITESM) for scientific discussions.

Notes and references

1 (*a*) S. Yang, G. S. B. Martin, G. J. J. Titman, A. J. Blake, D. R. Allan, N. R. Champness and M. Schröder, *Inorg. Chem.*, 2011, **50**, 9374–9384; (*b*) A. J. Nuñez, L. N. Shear, N. Dahal, I. A. Ibarra, J. W. Yoon, Y. K. Hwang, J.-S. Chang and S. M. Humphrey, *Chem. Commun.*, 2011, **47**, 11855–11857; (*c*) I. A. Ibarra, K. E. Tan, K. V. M. Lynch and S. M. Humphrey, *Dalton Trans.*, 2012, **41**, 3920–3923.

2 J. J. Low, A. I. Benin, P. Jakubczak, J. F. Abrahamian, S. A. Faheem and R. R. Willis, *J. Am. Chem. Soc.*, 2009, **131**, 15834–15842.

3 J. Cavinet, A. Feteeva, Y. Guo, B. Coasne and D. Farrusseng, *Chem. Soc. Rev.*, 2014, **43**, 5594–5617.

4 A. M. Ribeiro, T. P. Sauer, C. A. Grande, R. F. P. M. Moreira, J. M. Loureiro and A. E. Rodriguez, *Ind. Eng. Chem.*, 2008, **47**, 7019–7026.

5 (*a*) K. Sumida, D. L. Rogow, J. A. Mason, T. M. McDonald, E. D. Bloch, Z. R. Herm, T.-H. Bae and J. R. Long, *Chem. Rev.*, 2011, **112**, 724–781; (*b*) R. S. Haszeldine, *Science*, 2009, **325**, 1647–1652.

6 J. H. Cavka, S. Jakobsen, U. Olsbye, N. Guillou, C. Lamberti, S. Bordiga and K. P. Lillerud, *J. Am. Chem. Soc.*, 2008, **130**, 13850–13851.

7 H. A. Lara-García, M. R. Gonzalez, J. H. González-Estefan, P. Sánchez-Camacho, E. Lima and I. A. Ibarra, *Inorg. Chem. Front.*, 2015, **2**, 442–447.

8 K. A. Cychosz and A. J. Matzger, *Langmuir*, 2010, **26**, 17198–17202.

9 D.-Y. Hong, Y. K. Hwang, C. Serre, G. Férey and J.-S. Chang, *Adv. Funct. Mater.*, 2009, **19**, 1537–1552.

10 J. Liu, F. Zhang, X. Zou, G. Yu, N. Zhao, S. Fan and G. Zhu, *Chem. Commun.*, 2013, **49**, 7430–7432.

11 J. Qian, F. Jiang, D. Yuan, M. Wu, S. Zhang, L. Zhang and M. Hong, *Chem. Commun.*, 2012, **48**, 9696–9698.

12 W. M. Bloch, R. Babaro, M. R. Hill, C. J. Doonan and C. J. Sumby, *J. Am. Chem. Soc.*, 2013, **135**, 10441–10448.

13 P. M. Schoenecker, C. G. Carson, H. Jasuja, C. J. J. Flemming and K. S. Walton, *Ind. Eng. Chem. Res.*, 2012, **51**, 6513–6519.

14 J. Cavinet, J. Bonnefoy, C. Daniel, A. Legrand, B. Coasne and D. Farrusseng, *New J. Chem.*, 2014, **38**, 31012–33111.

15 H. Furukawa, F. Gándara, Y.-B. Zhang, J. Jiang, W. L. Queen, M. R. Hudson and O. M. Yaghi, *J. Am. Chem. Soc.*, 2014, **136**, 4369–4381.

16 (*a*) F. Meunier, *Appl. Therm. Eng.*, 2013, **61**, 830–836; (*b*) C. Janiak and S. K. Henninger, *Chimia*, 2013, **67**, 419–424.

17 M. Sadakiyo, H. Ōkawa, A. Shigematsu, M. Ohba, T. Yamada and H. Kitagawa, *J. Am. Chem. Soc.*, 2012, **134**, 5472–5475.

18 (*a*) S.-i. Noro, R. Matsuda, Y. Hijikata, Y. Inubushi, S. Takeda, S. Kitagawa, Y. Takahashi, M. Yoshitake, K. Kubo and T. Nakamura, *ChemPlusChem*, 2015, **80**, 1517–1524; (*b*) D. Kim, Y.-H. Ahn and H. Lee, *J. Chem. Eng. Data*, 2015, **60**, 2178–2186; (*c*) J. A. Mason, T. M. McDonald, T.-H. Bae, J. E. Bachman, K. Sumida, J. J. Dutton, S. S. Kaye and J. R. Long, *J. Am. Chem. Soc.*, 2015, **137**, 4787–4803.

19 (*a*) J. Liu, A. I. Benin, A. M. B. Furtado, P. Jakubczak, R. R. Willis and M. D. LeVan, *Langmuir*, 2011, **27**, 11451–11456; (*b*) J. Liu, Y. Wang, A. I. Benin, P. Jakubczak, R. R. Willis and M. D. LeVan, *Langmuir*, 2010, **26**, 14301–14307.

20 A. C. Kizzie, A. G. Wong-Foy and A. J. Matzger, *Langmuir*, 2011, **27**, 6368–6373.

21 (*a*) H. Jasuja, Y.-G. Huang and K. S. Walton, *Langmuir*, 2012, **28**, 16874–16880; (*b*) H. Jasuja, J. Zang, D. S. Sholl and K. S. Walton, *J. Phys. Chem. C*, 2012, **116**, 23526–23532; (*c*) J. B. DeCoste, G. W. Peterson, H. Jasuja, T. G. Glover, Y.-G. Huang and K. S. Walton, *J. Mater. Chem. A*, 2013, **1**, 5642–5650; (*d*) N. C. Burtch, H. Jasuja and K. S. Walton, *Chem. Rev.*, 2014, **114**, 10575–10612.

22 E. Soubeyrand-Lenoir, C. Vagner, J. W. Yoon, P. Bazin, F. Ragon, Y. K. Hwang, C. Serre, J.-S. Chang and P. L. Llewellyn, *J. Am. Chem. Soc.*, 2012, **134**, 10174–10181.

23 G. E. Cmarik, M. Kim, S. M. Cohen and K. S. Walton, *Langmuir*, 2012, **28**, 15606–15613.

24 (*a*) I. A. Ibarra, S. Yang, X. Lin, A. J. Blake, P. J. Rizkallan, H. Nowell, D. R. Allan, N. R. Champness, P. Hubberstey and M. Schröder, *Chem. Commun.*, 2011, **47**, 8304–8306; (*b*) M. R. Gonzalez, J. H. González-Estefan, H. A. Lara-García, P. Sánchez-Camacho, E. I. Basaldella, H. Pfeiffer and I. A. Ibarra, *New J. Chem.*, 2015, **39**, 2400–2403.

25 (*a*) X. B. Zhao, B. Xiao, A. J. Fletcher, K. M. Thomas, D. Bradshaw and M. J. Rosseinsky, *Science*, 2004, **306**, 1012–1015; (*b*) H. J. Choi, M. Dincă and J. R. Long, *J. Am. Chem. Soc.*, 2008, **130**, 7848–7850.

26 V. Haigis, F.-X. Coudert, R. Vuilleumier and A. Boutin, *Phys. Chem. Chem. Phys.*, 2013, **15**, 19049–19056.

27 I. P. O'koye, M. Benham and K. M. Thomas, *Langmuir*, 1997, **13**, 4054–4059.

28 (*a*) N. L. Ho, F. Porcheron and R. J.-M. Pellenq, *Langmuir*, 2010, **26**, 13287–13296; (*b*) L. N. Ho, J. Perez-Pellitero, F. Porcheron and R. J.-M. Pellenq, *Langmuir*, 2011, **27**, 8187–8197; (*c*) L. N. Ho, S. Clauzier, Y. Schuurman, D. Farrusseng and B. Coasne, *J. Phys. Chem. Lett.*, 2013, **4**, 2274–2278.

29 R. A. Peralta, B. Alcántar-Vázquez, M. Sánchez-Serratos, E. González-Zamora and I. A. Ibarra, *Inorg. Chem. Front.*, 2015, **2**, 898–903.

30 G. R. Medders and F. Paesani, *J. Phys. Chem. Lett.*, 2014, **5**, 2897–2902.

31 C. Serre, F. Millange, C. Thouvenot, M. Noguès, G. Marsolier, D. Louer and G. Férey, *J. Am. Chem. Soc.*, 2002, **124**, 13519–13526.

